EINSTEIN Observations of T Tauri Stars in Taurus-Auriga. I: Properties of X-Ray Emission

F. Damiani, G. Micela, S. Sciortino
Istituto ed Osservatorio Astronomico di Palermo,
Piazza del Parlamento 1,
90134 Palermo, Italy

F.R. Harnden, Jr.
Harvard-Smithsonian Center for Astrophysics,
60 Garden Street,
Cambridge, MA 02138, USA

Abstract

We present a systematic reanalysis of the *Einstein* IPC X-ray data on the pre-main-sequence stars in the Taurus-Auriga star-formation region. We consider all catalogued stars in this region which have been observed with the IPC; of these, 52 out of 68 can be identified with X-ray sources; upper limits on the X-ray luminosity have been evaluated in the remaining cases. We derive an X-ray luminosity function, and argue that its median L_x is representative of the population intrinsic value, in spite of incompleteness of the sample and possible ambiguities in the X-ray source identifications. As a result, it is confirmed that the known steady increase in the average level of X-ray emission toward younger ages can be extended to the pre-main-sequence phase. By using the line equivalent width as the relevant parameter, a statistically significant difference is found between the distributions of X-ray luminosities of stars with and without strong emission lines. No such difference is found instead between stars with and without strong infrared excess at 25μ.
Subject headings: stars: pre-main-sequence – X-rays: stars

1. Introduction

Pre-main-sequence (PMS) stars have long been known to exhibit peculiar spectral characteristics at almost all wavelengths with respect to ordinary late-type main-sequence stars (see e.g. the review by Bertout 1989). Excesses in the line and continuum emission are commonly detected, and have therefore been used to identify these stars spectroscopically. Strong emission lines of hydrogen and other elements are usually observed (Cohen & Kuhi 1979), with equivalent widths much above those of dKe-dMe stars, and are well explained by stellar wind models (e.g. Hartmann et al. 1990). In particular, the observations made with the *Einstein Observatory* showed that the emission at X-ray wavelengths of some T Tauri stars is several orders of magnitude enhanced with respect to that of main-sequence stars of similar spectral types, and the same result is currently being obtained from ROSAT observations.

In the last fifteen years, our knowledge of the X-ray emission from normal stars has increased substantially, mainly on the basis of the data collected with *Einstein* (Vaiana et al. 1981, Rosner, Golub and Vaiana 1985, Vaiana et al. 1992, Sciortino 1993, and references therein). It turned out that X-ray emission is detected almost everywhere throughout the HR diagram, with the possible exception of late B/early A dwarfs and late K and M supergiants. The observed connection between X-ray emission and stellar rotation for late-F to M stars has suggested a dynamo mechanism for its origin in these stars, in analogy with the Sun (cf. Rosner & Vaiana 1979).

The average stellar X-ray luminosity of solar-like stars is also known to increase toward younger ages, passing from field stars to the Hyades, Pleiades and up to the very young pre-main-sequence stars (Caillault & Helfand 1985, Micela et al. 1985, 1988, 1990, Feigelson & Kriss 1989). In fact, the spatial density of X-ray sources in regions of star formation is higher than the average density over the whole sky since the typical X-ray emission of young stars is high (Montmerle et al. 1983, Feigelson et al. 1987, Walter et al. 1988).

However, systematic studies of X-ray emission are limited to some star-formation regions, like the Chamaeleon region (Feigelson & Kriss 1989), and the Orion B (L1641) cloud (Strom et al. 1990), while for other regions, such as Taurus-Auriga, published papers refer only to subsets of all available data, (and were mostly based on early reductions (REV 0) of *Einstein* data). Also the contribution from ROSAT observations of Tau-Aur stars is, at present, limited to some star-forming clouds in the region (L1495E, Strom & Strom 1994).

X-ray observations of small samples of T Tauri stars in Taurus-Auriga have been presented by Gahm (1980), Feigelson & DeCampli (1981), Feigelson & Kriss (1981), Walter & Kuhi (1981, 1984). A number of stars were detected with the Imaging Proportional Counter (IPC) of the *Einstein* satellite, with X-ray luminosities $L_x \sim 10^{30} - 10^{31}$ ergs/sec. Since flarelike variability was identified only in a small fraction of the X-ray detected stars, most of the detected X-ray flux arises from a quiescent component (Feigelson & DeCampli 1981, Walter & Kuhi 1984).

Emission from shocks in circumstellar envelopes is hardly compatible with both the observed X-ray luminosity and typical energies ($\geq$1 keV; Feigelson & DeCampli 1981); rather, the rapid variability sometimes observed (Feigelson & DeCampli 1981, Walter & Kuhi 1984; see also Montmerle et al. 1983 about the ρ Oph star-forming region) suggests that the X-ray emitting regions are fairly small, and close to the photosphere. Feigelson & Kriss (1981) argue that this X-ray emission is similar in character to that of main-sequence stars, although scaled up by factors of $\sim 10^3$.

In several star-forming regions, the IPC observations also led to the identification of many new PMS stars, previously unnoticed due to their weak emission-line activity (Walter & Kuhi 1981, Feigelson & Kriss 1981, Mundt et al. 1983, Walter 1986, Feigelson et al. 1987, Walter et al. 1987, 1988). The studies later than about 1985 made use of the latest revision of IPC data (REV 1), but no reanalysis of the early data on well-known classical T Tauri stars was included, nor was a detailed comparison made between the X-ray properties of the latter and the newly discovered PMS stars.

Therefore, it seemed to us worthwhile to systematically reanalyze the whole *Einstein* X-ray dataset provided by the REV 1 release (Harnden et al. 1984), concerning PMS stars in the

Taurus-Auriga region (the nearest large star-formation region). By considering together stars having widely different levels of activity, we will take advantage of a broader dynamical range, as compared to previous works, over which to study the unclear relationships between the X-ray- and line emission in these stars.

The paper is structured as follows: section 2 is a description of the observations, data selection and reduction; in section 3 the average X-ray properties of various subsamples are tested by the use of X-ray luminosity functions; the main results obtained are summarized in section 4.

2. Data Selection and Analysis

2.1 *The Observed Sample*

Our sample is composed of all PMS stars in the Taurus-Auriga star formation region as listed in the Herbig & Bell (1988) catalog of emission-line stars of the Orion Population (hereafter HBC), and which have been observed in X-rays with the *Einstein* Observatory. The HBC is an update of the Herbig & Rao (1972) catalog, and most of the new catalog entries are stars which exhibit a general activity far less intense than classical T Tauri stars (CTTS), and which have been named weak-lined T Tauri stars (WTTS). Due to the different techniques used in selecting various classes of stars, the homogeneity and completeness of the catalog is not guaranteed, as explicitly stated by the authors themselves. Most WTTS have been selected as PMS stars as a result of searches for emission in the Ca II H and K lines (Herbig, Vrba & Rydgren 1986), or for strong X-ray sources in regions of stellar formation (Walter 1986, Walter et al. 1988), and our WTTS sample is therefore biased towards bright X-ray sources. We have however attempted to build an *unbiased* WTTS sample, made of all WTTS not originally selected as X-ray sources, and we have compared results obtained from this small subsample with those derived for the whole WTTS sample.

Due to the difficulty of distinguishing a star near the end of its pre-main-sequence phase (or with low line emission anyway) from a very young main-sequence star, and since possible main-sequence stars have been conservatively excluded from the HBC, the catalog should be quite incomplete for stars in their latest pre-main-sequence stages. Indeed, despite the variety of techniques used to find stars in this evolutionary stage, the known stars with estimated ages of $\sim 10^7$ yr have remained much less numerous than expected (Kenyon & Hartmann 1990; Herbig, Vrba & Rydgren 1986).

In this respect we note that recently Favata et al. (1993), analyzing the lithium abundance in a sample of G and K coronal sources selected from the X-ray-flux limited Extended Medium Sensitivity Survey (Gioia et al. 1990, Stocke et al. 1991) have shown that a sizeable fraction of high-latitude ($|b| > 20°$) coronal sources outside of 'classical' star-formation regions are indeed young or pre-main-sequence stars.

We define the Tau-Aur region as the sky region within $3^h0^m0^s <$ RA $< 5^h5^m0^s$ and $+15° <$ Dec $< +40°$; 160 HBC stars fall inside this region[1] (Figure 1). They are distributed highly nonuniformly across the region, except for the weak-lined T Tauri stars, which, as already noted by Walter et al. (1988), keep generally at a greater distance from the cloud center.

From the previously defined sample we have extracted all stars which have been observed in X-rays with the *Einstein* Observatory (Giacconi et al. 1979); the IPC (Gorenstein, Harnden & Fabricant 1981) was the only instrument on this satellite which observed stars of our sample, in the energy band 0.16-3.5 keV.

It is worthwhile to note how a certain degree of inhomogeneity in the optical sample, containing stars selected in various ways (Hα, Ca II, X-ray emission) affects our study of X-ray emission properties: stars selected through Hα (or Ca II H&K) emission are an unbiased sample with respect to X-ray emission. This is not true for X-ray selected stars, which constitute most of known WTTS, as noted, and for which the L_x distribution we derive may describe, in principle, only the high-L_x tail of their true distribution. However, the existence of a large number of unknown WTTS below our detection threshold is not suggested by the L_x distribution of WTTS selected independently of X-rays (see section 3.1). A caveat is in order, anyway, since this latter

[1] We have however excluded from the sample star Wa Tau/1 (HBC 408), since this was considered not a PMS star by Walter (1986).

sample may not be entirely unbiased with respect to X-rays: in fact, these stars were selected on the basis of their Hα or Ca II emission, which are shown to correlate with X-ray emission in the case of WTTS (Paper II).

In Figure 1 we show all the IPC fields in the Taurus region (squares), together with all PMS stars of the optical sample (dots); it is seen that only a small fraction of the region is covered by the X-ray observations. In total, 71 stars of our optical sample, contained in 34 distinct IPC fields, have been observed by *Einstein*. We have verified that the distributions of spectral types in this sample is nearly identical to that of the optical sample, and therefore is not affected by the incomplete sampling of the X-ray observations (Figure 2*a*) (a Pearson's χ^2 test (Eadie et al. 1971) applied to the two distributions gives a probability of only $P = 17\%$ of not being drawn from the same parent population). The same holds for the distribution of levels of atmospheric activity, as indicated by the $H\alpha$ line equivalent width (Figure 2*b*), with a χ^2 test probability of $P = 24\%$. A comparison of the visual magnitude distributions of the optical and X-ray samples, gives instead some indication that these distributions may be different, with a probability of $P = 95\%$. A visual inspection of the two distributions (Figure 2*c*) suggests that this difference arises because stars fainter than about $m_V < 13$ are less represented in the X-ray sample, with respect to the optical sample. The V magnitudes, spectral types and Hα equivalent widths are taken from the Herbig & Bell (1988) catalog.

2.2 *X-Ray Observations*

The identification of the sample stars with the X-ray sources in the field, and the analysis of the X-ray data have been done uniformly over the whole sample, by using the latest version of the IPC data reduction system (REV 1, Harnden et al. 1984); improvements with respect to the early (REV 0) IPC data release consist of a more accurate instrument gain, and a higher sensitivity due to improved background maps. The REV 1 data for our sample stars are in many cases different from the REV 0 ones, primarily because the low signal-to-noise ratio of most detected sources makes the derivation of accurate count rates very sensitive to details of the data reduction process, such as the screening of data from various contaminations. Figure 3 is a plot of L_x derived in this work versus L_x values reported in literature. As this figure makes it evident, apart from a scatter of a factor 3, in a non-negligible number of cases the difference between REV 1 and REV 0 derived L_x is even larger. An extreme case is that of DG Tau, for which Feigelson & DeCampli (1981) reported a large X-ray flare, while REV 1 data of the same IPC observation do not even show a source at the stellar position, but only a constant X-ray background. We have therefore chosen to carry out the X-ray data analysis for these stars independently of previously published works. In particular, the homogeneous data reduction procedure for both CTTS and WTTS allows a careful comparison of their respective X-ray properties.

The REV 1 system uses two distinct methods to detect X-ray sources in each image, namely the 'Map' and 'Local' methods (differing in the evaluation of the X-ray background, see e.g. Micela et al. 1988), each one applied in the 'soft' (0.16-0.8 keV), 'hard' (0.8-3.5 keV) and 'broad' (0.16-3.5 keV) IPC spectral bands.

The spatial resolution varies with observed pulse height, but is always better than $3'$. We have cross-checked the optical positions of all stars in the X-ray sample with the positions of all X-ray sources in Tau-Aur. We found that 53 stars fall within the ($3'$ radius) circles centered on X-ray sources, corresponding to 38 distinct X-ray sources (16 out of these 38 sources are observed more than once). In 24 cases there is a single star of our sample within $3'$ of the corresponding X-ray source: we shall occasionally refer to these stars as 'single identifications'. In addition, we found 13 pairs and a group of three stars of the sample within $3'$ of the corresponding X-ray sources ('multiple identifications'); these are the pairs RY Tau/LkCa 21, DH/DI Tau, UX Tau A/B, V710 Tau A/B, GH/V807 Tau, GI/GK Tau, AB/SU Aur, RW Aur A/B, NTTS 035120+3154 SW/NE, NTTS 035135+2528 NW/SE, NTTS 040012+2545 S/N, NTTS 040047+2603 W/E, NTTS 040142+2150 SW/NE, and the group HL Tau, XZ Tau, LkHα 358. In these cases the IPC data alone cannot indicate what fraction of the observed counts is contributed from each star.

In one case it seemed possible to refine the identification made. The stars AB Aur and SU Aur are identified with the same X-ray source, and their offsets between X-ray and optical positions are $\sim 2'.7$ and $\sim 0'.3$, respectively. Therefore, taking also into account their small off-axis position in the IPC image, and the large number of recorded X-ray photons, which reduces the positional error, we have identified uniquely the X-ray source with SU Aur, treating AB Aur as not detected in X-rays. This reduces the number of stars having an X-ray counterpart more distant than $1'$ to only two. We then obtain that, out of 71 stars observed in X-rays by *Einstein*, 52 are identified with X-ray sources, and we have evaluated upper limits to the X-ray luminosity of the remaining 19 stars.

The standard IPC data reduction system gives, for each detected X-ray source (for each detection method and spectral band), the value of background-corrected recorded count rate (Harnden et al. 1984). To preserve maximum uniformity in the data analysis of our whole sample, we have chosen to use the data obtained with the 'Map' method in the broad band, which detects the greatest number of objects in our sample; only three objects are detected exclusively by the 'Local' method, or by the 'Map' method in other spectral bands. In these latter three cases, we used count rates given by the 'Local' method, in the same broad energy band.

For optical stars observed and detected in more than one IPC field (16 distinct X-ray sources in our sample), we have chosen to ignore those detections affected by the detector supporting structure and edges, since they are of much poorer quality. This procedure results in a single count rate for the X-ray source identified with each star, except for five stars: three of these are single identifications, and the remaining pair is identified with a single X-ray object, so in total we have four X-ray objects, each observed twice. In these cases we have chosen to adopt a 'maximum likelihood' procedure (Sciortino & Micela 1992) to assign a single count rate to each given X-ray object (obtained as a weighted mean, according to the statistical errors, of the values given by each observation)[2].

The count rates can be transformed into observed fluxes (between 0.16 and 3.5 KeV) using a conversion factor (Harris et al. 1993), computed for the IPC broad band by assuming a Raymond thermal spectrum (Raymond & Smith 1977), and depending on the source temperature and on the line-of-sight hydrogen column density N_H. Taking advantage of the spectral resolution of the IPC, one can define the Hardness Ratio, HR, as

$$\mathrm{HR} = \frac{\mathrm{counts(hard\ band)} - \mathrm{counts(soft\ band)}}{\mathrm{counts(hard\ band)} + \mathrm{counts(soft\ band)}}.$$

Hardness ratios for our X-ray sources are generally quite higher than those observed for main-sequence stars, in agreement with previous work (Feigelson & Kriss 1981, Walter & Kuhi 1981, 1984), apparently indicating quite high temperatures for the X-ray emitting plasma of PMS stars. However, since these HR are in most cases affected by large errors, they cannot be reliably used to deduce temperature values. We have instead performed spectral fits on the two sample stars with the largest number of X-ray counts (SU Aur, HD 283572) using the IRAF/PROS spectral package, which yielded temperatures of 1.1 [1.0-1.5] keV, and 1.5 [1.1-2.3] keV, respectively; the result for HD 283572 is compatible with the value of 2.2 [1.1->15] keV reported by Schrijver, Mewe and Walter (1984), as well as with the detailed analysis of the X-ray spectrum of this star made by Walter et al. (1987). The mean of the two temperatures we derive (1.3 keV, corresponding to $T = 1.5 \cdot 10^7$ K), is compatible with the HR observed for the other sample stars, and therefore we have assumed this temperature for all stars of the sample. For T higher (lower) by a factor of two, the error in the conversion factor would be +13.8% (-8.9%) for a typical $N_H = 1.4 \cdot 10^{21}\mathrm{cm}^{-2}$, and -16.2% (+105.0%) for a quite extreme value of $N_H = 7.7 \cdot 10^{21}\mathrm{cm}^{-2}$. The value of N_H is estimated

[2] The validity of the procedure may be questioned if the individual values of count rate differ beyond the 3σ value, because this would indicate intrinsic X-ray variability. This happens only for AA Tau among the objects considered here, detected twice with count rates of 0.024 ± 0.005, and 0.005 ± 0.001 cts/sec, respectively. However, since we lack details of its X-ray lightcurve, we have applied the maximum-likelihood procedure even in this case. There is no clear evidence that the larger X-ray count rate has to be ascribed to a large flare, since the X-ray lightcurve at X-ray maximum, as derived by us from REV 1 data, is flat over the observation time span of 2032 seconds. Of course, further studies on the nature of X-ray variability in T Tauri stars are warranted.

for the individual stars from the optical extinction A_V, assuming for the entire line of sight a mass ratio between neutral hydrogen and dust equal to the average interstellar ratio, and making use of the relation: $N_H = 2.22 \cdot 10^{21} \cdot A_V$ cm^{-2} (Gorenstein 1975). The values for the optical extinction are taken from Cohen & Kuhi (1979), and Strom et al. (1989). An error by a factor of two higher (lower) in the value of N_H about the estimated values, and for the temperature range of our interest, results in an error in the conversion factor of +35.0% (-16.1%). For the stars without a published extinction value we adopted an average conversion factor of $3.41 \cdot 10^{-11}$ergs cm^{-2} count^{-1} (corresponding to $N_H = 1.4 \cdot 10^{21}$ cm^{-2}). The evaluation of uncertainties on the values of N_H is difficult, not only because A_V values from different authors may easily differ by $\sim$1 mag, but also since the adopted proportionality between N_H and A_V might not hold in a T Tauri star circumstellar environment. For example, a hot, dust-free wind will contribute only to N_H, but not to the optical extinction A_V. Using N_H as given by X-ray spectral fits on HD 283572 and SU Aur we derive N_H/A_V ratios of 9.6 [6.1-27.2] $\cdot 10^{20}$ and 6.9 [3.4-7.6] $\cdot 10^{21}$ cm^{-2} mag^{-1}, respectively, which brackett the interstellar value and are compatible with it within the 3σ level. The reliability of the absorption corrections we have applied will also be discussed in a companion paper (Damiani & Micela 1994, henceforth Paper II), in connection with the correlations of X-ray emission with stellar properties.

Assuming all stars to be at the distance of the Tau-Aur complex (140 pc), we then obtain a value of L_x for each source. Given the sky-projected extension of the cluster ($\sim$ 20 pc) we estimate an error of 14% on L_x, on the basis of the lack of individual distance values alone. Taking into account all sources of uncertainty, the typical overall uncertainty on L_x is 55% (rising to 65% for the lowest signal-to-noise detections), and is mainly due to the poor knowledge of N_H (and A_V).

In the case of multiple identifications, we have divided equally the observed counts between the optical counterparts. This approach gives 'maximum likelihood' X-ray luminosities, if we lack a valid criterion to split the observed count rate among counterparts. Since we will present in Paper II various dependences of L_x on bolometric luminosity, rotation rate, and Hα emission (holding for various subsamples), it is not clear which criterion should be applied in each case. This is a fundamental problem of all low-spatial resolution detectors, and cannot be solved until higher-resolution observations will be available. Since it affects about half of our sample, we will treat distinctly single- from multiple identifications, to check to what extent the identification problem affects the correlations found (Paper II).

Alternatively, since Walter et al. (1988) found that the X-ray surface flux is roughly constant during the PMS phase, one could split count rates in proportion to the squared stellar radii, or to bolometric luminosities. This approach would yield L_x values significantly different from those we have derived only for a few stellar pairs whose components are quite different, like RW Aur A/B or UX Tau A/B. For these cases, the X-ray luminosity of the primary would increase by a factor of 2 with respect to the value we have derived. Given the overall uncertainty on L_x, this would not sensibly affect any of our conclusions.

2.3 *The Undetected Stars*

In addition to the stars identified with X-ray sources, we consider also those observed by the IPC but undetected in X-rays in any band by any method. There are 19 such stars in our sample. However, three of them fell behind detector ribs, and were therefore discarded from our sample as not having been observed. Among these, the star HBC 412 deserves a special mention: this star falls at $\sim 2'.3$ distance from *two* distinct X-ray detections *in the same IPC image*. Because these sources are only detected with the 'Map' method, are quite far ($\sim 30'$) from the telescope axis, and are strongly obscured by the detector ribs, we could not derive even an approximate X-ray count rate for this star, and we have omitted it altogether from our sample, despite its likelihood of being an X-ray emitter. We are thus left with 16 stars for which we calculate an upper limit to L_x. We have followed the prescriptions of Harris et al. (1993) which allow us to obtain 3.5σ

limiting count-rate values, knowing the star position relative to a specified IPC image, and the exposure time of the latter.

Once an upper limit to the recorded count rate was obtained in this way for each undetected star, we proceeded as for detections to get a limiting value for L_x, using a value of N_H derived from A_V, and assuming the same temperature as adopted for detections. The X-ray data for all stars in the observed sample are summarized in Table 1*a*, *b*, together with other relevant data taken from literature. The quantity η whose correlation with L_x is extensively discussed in Paper II, is reported here for completeness.

3. Results and Discussion

3.1 *The Level of X-Ray Emission in Taurus-Auriga*

We have analyzed the X-ray data obtained for the Tau-Aur T Tauri stars by computing maximum-likelihood X-ray luminosity functions, a method often employed to examine distributions of quantities including upper limits, and therefore well suited for our X-ray data (see Avni et al. 1980, Schmitt 1985, Feigelson & Nelson 1985). The X-ray luminosity function for our stars is shown as the solid line in Figure 4; we see that L_x ranges from $10^{29.5}$ to $10^{31.4}$ ergs/sec, with the lower value set by the instrument sensitivity threshold. The median of $\log L_x$ is 29.82 [+0.08,-0.06], and its mean 29.91 [+0.04,-0.04], where the 1σ errors were computed using a 'bootstrap' procedure with 200 iterations (cf. Schmitt 1985). Having detected as X-ray sources *at least* 38 stars out of 68 (this number is obtained by considering as detected only one star for each multiple identification), the measured median L_x for our sample is at first sight representative of the entire Tau-Aur PMS population; however, this might be a result of the sample composition.

If we restrict ourselves to the group of the CTTS alone, we detect at least 17 (and up to 26) stars out of 42 (the ambiguity is again due to the problem of the multiple identifications). We separate here CTTS from WTTS on the basis of their detection at 25μ, which is a better proxy than Hα emission to sample circumstellar activity. With the percentage of detections ranging from 40% to 62%, we are not entirely sure of having reached the median, whose true value might therefore be slightly lower than the one we calculate (median $\log L_x$=29.74 (ergs/sec)) for the CTTS alone. On the other hand, in the case of the WTTS we have 81% to 100% detected stars, which is simply a result of the sample composition; therefore also in this case the true median X-ray luminosity is likely to be lower than the obtained value of median $\log L_x$=29.93 (ergs/sec). There are reasons, anyway, to think that the average X-ray luminosity is not far from this value, even for WTTS, since if we restrict to consider only the WTTS discovered independently from X-ray observations (V807 Tau, NTTS 042950+1757, NTTS 042916+1751, LkCa 19, NTTS 041636+2743; Walter et al. 1988, Feigelson & Kriss 1983), we find a median $\log L_x$ =29.9.

In Figure 4, we have compared the total sample L_x maximum-likelihood distribution with analogous distributions already obtained by various authors for the Chamaeleon star-formation region (Feigelson & Kriss 1989), the Pleiades K-M stars (Micela et al. 1990), the Hyades K-M stars (Micela et al. 1988), the young and old disk K-M stars (Barbera et al. 1993). The fact that in Figure 4 the Tau-Aur and Chamaeleon luminosity functions intersect should be not surprising. The low-luminosity region of the Tau-Aur luminosity function is populated due to a few deep IPC exposures, which were not available for Chamaeleon stars. The high-L_x tail of the Tau-Aur luminosity function is populated by only two stars, which scaled to the smaller Chamaeleon sample size is compatible with zero detected stars at this high L_x value.

We also report in Figure 5 the median X-ray luminosities of these samples as a function of the stellar age. Vertical bars indicate the 16-84% quantile range of L_x, approximately describing the (1σ) dispersion for each stellar sample. As is seen in the Figure, the range of X-ray luminosities in Tau-Aur turns out to be nearly the same as in Chamaeleon. Therefore, our study of Tau-Aur PMS stars suggests that the decrease of X-ray luminosity of late-type stars with increasing stellar age can be definitely extended to the PMS phase of evolution, confirming results based on previous works (e.g. Feigelson & Kriss 1989). We find that the range of L_x for stars in stellar formation regions such as Tau-Aur is at least two orders of magnitude, hence some parameters other than age have to be invoked in order to explain it.

We should note also that the Chamaeleon region has been recently observed with the ROSAT PSPC, and a new estimate of its X-ray luminosity function is now available (Feigelson et al. 1993). The main differences with respect to the IPC luminosity function of Feigelson & Kriss (1989) are its extension towards lower X-ray luminosities, and the depletion of part of its high-luminosity tail, as a consequence of the higher sensitivity and spatial resolution of the PSPC, respectively. Indeed, some strong IPC sources were resolved in many weaker components with the ROSAT PSPC. Differences in the performances of the two instruments, however, make of dubious validity a direct comparison of IPC and PSPC luminosity functions, as also Feigelson et al. (1993) note. Although the PSPC luminosity function is undoubtedly a better estimate of the true L_x distribution in Chamaeleon, we have therefore preferred to compare our results with the older IPC data (Feigelson & Kriss 1989) for this star-formation region.

3.2 *X-Ray Emission Levels for Different Classes of Stars*

In order to get some insight into the nature of the X-ray emission of our sample stars, we have compared the average X-ray emission levels of subsamples having different properties. Since PMS stars are characterized by optical emission lines and IR excesses, we have examined if these diagnostics are related to the observed X-ray activity. First, we have separated stars having $EW(H\alpha)$ greater and less than 10 Å, respectively. The corresponding X-ray luminosity functions for these two subsamples are plotted and compared in Figure 6. To confirm the difference apparent from the figure, we applied a Wilcoxon test (Feigelson & Nelson 1985) to the two distributions and found that the null hypothesis (that they are drawn from the same parent population) is rejected at the 99.67% confidence level.

This result should however be interpreted with caution: as noted in section 2.1, most (about 70%) stars having $EW(H\alpha) < 10$ Å have just been discovered through X-ray observations, and their X-ray luminosity function might be therefore biased towards high L_x values. In order to reduce this bias, although with the caveat of section 2.1, we considered only the (ten) stars both having $EW(H\alpha) < 10$ Å, and identified as pre-main-sequence objects independently from their X-ray emission (DI Tau, UX Tau A/B, SU Aur, V710 Tau B, IQ Tau, NTTS 042950+1757, NTTS 042916+1751, LkCa 19, and NTTS 041636+2743): their L_x distribution appears indistinguishable from that of the whole sample with $EW(H\alpha) < 10$ Å, possibly indicating that our previous result is not to be biased by the inclusion of X-ray selected stars. We conclude that stars having $EW(H\alpha)$ respectively larger and smaller than 10 Å have, on the average, different L_x.

We have also evaluated X-ray luminosity functions for CTTS and WTTS separated according to their IR emission (Figure 7). Here we have separated stars which were detected at 25μ by the satellite IRAS (Harris, Clegg & Hughes 1988, Strom et al. 1989) from those which were not; this amounts to fixing a threshold log $L_{25\mu} = 31.25$ (ergs/sec, emitted in the 16-30μ band) at the Tau-Aur distance (for a limiting observed flux of 0.1 Jy), a value which arises in a natural way, since almost all upper limits on $L_{25\mu}$ lie below it, while all detections are clearly above (cf. Table 1; see also Skrutskie et al. 1990, and Paper II). In this case the two classes only differ at the 62% confidence level, and by choosing the detectability at 12μ rather than at 25μ as the separating criterion, the confidence level drops to only 53%, i.e. they are indistinguishable. Therefore, we find that stars with very different far-IR emission exhibit indistinguishable X-ray behaviour.

It is worth noting that the two classifications we have made are quite similar to each other, since most stars detected at 25μ have $EW(H\alpha) > 10$ Å (Strom et al. 1989). The different behavior of the average X-ray luminosity as a function of IR emission and Hα equivalent width, respectively, suggests therefore that we are looking at subtle effects (yet statistically significant). This problem deserves further investigation, also at the light of current models of T Tauri stars, and it will be examined in Paper II.

4. Summary

We have reanalyzed all available *Einstein* IPC X-ray data on the PMS population of the Taurus-Auriga star formation region in a systematic way, on the basis of REV 1 IPC data. We derive X-ray luminosities and upper limits uniformly for both strong- and weak-line T Tauri populations of the cluster, and discuss how representative the studied sample is. Some of our findings are in qualitative agreement with previous studies, confirming them on a more sound statistical basis.

Our main results are:

1. A maximum-likelihood X-ray luminosity function has been built, including X-ray undetected stars, for the whole known pre-main-sequence population in Taurus-Auriga.

2. The X-ray luminosity distribution of T Tauri stars in Tau-Aur allows us to evaluate the median $\log L_x \sim 29.7$ (ergs/sec), at least for stars selected independently from their X-ray emission, although higher spatial resolution and a lower detection threshold are required to better constrain the median L_x.

3. The average level of X-ray emission in Tau-Aur turns out to follow the trend of decreasing X-ray luminosity with age, known for main-sequence young stars, as already found for the T Tauri population of the Chamaeleon star-forming region.

4. Using the Hα equivalent width as a separating criterion, a significant difference is found between the X-ray luminosity distributions of strong- and weak-emission line stars.

5. Separating the subsamples of stars having infrared emission at 25μ higher and lower than a threshold of $\log L_{25\mu} = 31.25$ ergs/sec (0.1 Jy), no significant difference exists between their X-ray luminosity distributions.

6. The IPC X-ray spectra of two stars with highest number of X-ray counts (SU Aur and HD 283572) are well fitted by Raymond-Smith thermal spectra, with temperatures of 1.1 [1.0-1.5] keV, and 1.5 [1.1-2.3] keV, respectively.

This work was inspired by the late G.S.Vaiana, who took part in its early development and without whose contributions this paper might never have been.

We acknowledge support by the Italian Ministero per la Ricerca Scientifica e Tecnologica, and from Agenzia Spaziale Italiana (FD, GM, SS). FRH acknowledges partial support under NASA contract NAS8-30751. We are grateful to F.Reale, A.Maggio, A.Collura, and H.Tananbaum for useful discussions and comments on this paper, and to D.Randazzo for her help to improve the form of the original manuscript. We are also indebted to an anonymous referee and to T.Simon, whose suggestions have allowed us to improve significantly this paper.

REFERENCES

Avni,Y., Soltan,A., Tananbaum,H., Zamorani,G. 1980, ApJ 238, 800.

Barbera,M., Micela,G., Sciortino,S., Harnden,F.R.,Jr., Rosner,R. 1993, ApJ, 414, 846.

Bertout,C. 1989, Ann. Rev. Astron. Ap., 27, 351.

Bouvier,J., Bertout,C., Benz,W., Mayor,M. 1986, A&Ap, 165, 110.

Bouvier,J., Bertout,C. 1989, A&Ap, 211, 99.

Bouvier,J., Cabrit,S., Fernandez,M., Martin,E.L., Matthews,J.M. 1993, A&Ap, 272, 176.

Caillault,J.P., Helfand,D.J. 1985, ApJ, 289, 279.

Cohen,M., Kuhi,L.V. 1979, ApJS, 41, 743.

Cohen,M., Emerson,J.P., Beichman,C.A. 1989, ApJ, 339, 455.

Damiani,F., Micela,G. 1994, ApJ submitted (Paper II).

Eadie,W.T., Drijard,D., James,F.E., Roos,M., Sadoulet,B. 1971, Statistical Methods in Experimental Physics, North-Holland.

Favata,F., Barbera,M., Micela,G., Sciortino,S. 1993, A&Ap, 277, 428.

Feigelson,E.D., Kriss,G.A. 1981, ApJLett, 248, L35.

Feigelson,E.D., DeCampli,W.M. 1981, ApJLett, 243, L89.

Feigelson,E.D., Nelson,P.I. 1985, ApJ, 293, 192.

Feigelson,E.D., Jackson,J.M., Mathieu,R.D., Myers,P.C., Walter,F.M. 1987, AJ, 94, 1251.

Feigelson,E.D., Kriss,G.A. 1983, AJ, 88, 431.

Feigelson,E.D., Kriss,G.A. 1989, ApJ, 338, 262.

Feigelson,E.D., Casanova,S., Montmerle,T., Guibert,J. 1993, ApJ, 416, 623.

Gahm,G.F. 1980, ApJLett, 242, L163.

Giacconi,R., et al. 1979, ApJ, 230, 540.

Gioia,I.M., Maccacaro,T., Schild,R.E., Wolter,A., Stocke,J., Morris,S., Henry,J.P. 1990, ApJS, 72, 567.

Gorenstein,P. 1975, ApJ, 198, 95.

Gorenstein,P., Harnden,F.R., Fabricant,D.G. 1981, IEEE Nucl. Sci., NS-28, 869.

Harnden,F.R., Jr., Fabricant,D.G., Harris,D.E., Schwartz,J.1984, Smithsonian Ap. Obs. Spec. Rept., No. 393.

Harris,S., Clegg,P., Hughes,J. 1988, MNRAS, 235, 441.

Harris,D.E., et al 1993, The Einstein Observatory Catalog of IPC X-ray Sources, vol.1, NASA TM 108401.

Hartmann,L., Calvet,N., Avrett,E.H., Loeser,R. 1990, ApJ, 349, 168.

Herbig,G.H. 1962, Advances in Astron. and Astrophys., 1, 47.

Herbig,G.H., Rao,N.K. 1972, ApJ, 174, 401.

Herbig,G.H., Vrba,F.J., Rydgren,A.E. 1986, AJ, 91, 575.

Herbig,G.H., Robbin-Bell,K. 1988, Third Catalog of Emission-Line Stars of the Orion Population, Lick Obs. Bull. n. 1111.

Herbst,W., Booth,J.F., Chugainov,P.F., Zajtseva,G.V., Barksdale,W., Covino,E., Terranegra,L., Vittone,A., Vrba,F. 1986, ApJLett, 310, L71.

Herbst,W., Booth,J.F., Koret,D.L., Zajtseva,G.V., Shakhovskaya,N.I., Vrba,F.J., Covino,E., Terranegra,L., Vittone,A., Hoff,D., Kelsey,L., Lines,R., Barksdale,W. 1987, AJ, 94, 137.

Kenyon,S.J., Hartmann,L.W. 1990, ApJ, 349, 197.

Martin,E.L., Rebolo,R., Magazzù,A., Pavlenko,Ya.V. 1994, A&Ap, 282, 503.

Micela,G., Sciortino,S., Serio,S., Vaiana,G.S., Bookbinder,J., Golub,L., Harnden,F.R., Rosner,R. 1985, ApJ, 292, 172.

Micela,G., Sciortino,S., Vaiana,G.S., Schmitt,J.H.M.M., Stern,R.A., Harnden, F.R., Rosner,R. 1988, ApJ, 325, 798.

Micela,G., Sciortino,S., Vaiana,G.S., Harnden,F.R., Rosner,R., Schmitt,J.H.M.M. 1990, ApJ, 348, 557.

Montmerle,T., Koch-Miramond,L., Falgarone,E., Grindlay,J.E. 1983, ApJ, 269, 182.

Mundt,R., Walter,F.M., Feigelson,E.D., Finkenzeller,U., Herbig,G.H., Odell,A.P. 1983, ApJ, 269, 229.

Praderie,F., Simon,T., Catala,C., Boesgaard,A.M. 1986, ApJ, 303, 311.

Raymond,J.C., Smith,B.W. 1977, ApJS, 35, 419.

Red'kina,N.P., Zausaeva,O.G. 1987, Astron. Tsirk., 1523, 5.

Rosner,R., Vaiana,G.S. 1979, in Proc. Intl. School of Astrophysics, Erice, eds. G.Setti and R.Giacconi.

Rosner,R., Golub,L., Vaiana,G.S. 1985, Ann. Rev. Astron. Ap, 23, 413.

Rydgren,A.E., Zak,D.S., Vrba,F.J.,Chugainov,P.F., Zajtseva,G.V. 1984, AJ, 89, 1015.

Rydgren,A.E., Vrba,F.J., Chugainov,P.F., Shakhovskaya,N.I. 1985, BAAS, 17, 556.

Schmitt,J.H.M.M. 1985, ApJ, 293, 178.

Schrijver,C.J., Mewe,R., Walter,F.M. 1984, A&Ap, 138, 258.

Sciortino,S., Micela,G. 1992, ApJ, 388, 595.

Sciortino,S. 1993, in Physics of Solar and Stellar Coronae, eds. J.Linsky and S.Serio (Dordrecht:Kluwer), p.211.

Skrutskie,M.F., Dutkevitch,D., Strom,S.E., Edwards,S., Strom,K.M., Shure, M.A. 1990, AJ, 99, 1187.

Stocke,J.T. et al. 1991, ApJS, 76, 813.

Strom,K.M., Strom,S.E., Edwards,S., Cabrit,S., Skrutskie,M.F. 1989, AJ, 97, 1451.

Strom,K.M., et al. 1990, ApJ, 362, 168.

Strom,K.M., Strom,S.E. 1994, ApJ, 424, 237.

Vaiana,G.S., et al. 1981, ApJ, 245, 163.

Vaiana,G.S., Maggio,A., Micela,G., Sciortino,S. 1992, MemSAIt, 63, 545.

Vrba,F.J., Rydgren,A.E., Zak,D.S., Chugainov,P.F., Shakhovskaya,N.I. 1984, BAAS, 16, 998.

Vrba,F.J., Rydgren,A.E., Chugainov,P.F., Shakovskaya,N.I., Zak,D.S. 1986, ApJ, 306, 199.

Walter,F.M., Kuhi,L.V. 1981, ApJ, 250, 254.

Walter,F.M., Kuhi,L.V. 1984, ApJ, 284, 194.

Walter,F.M. 1986, ApJ, 306, 573.

Walter,F.M., Brown,A., Linsky,J.L., Rydgren,A.E., Vrba,F., Roth,M., Carrasco,L., Chugainov,P.F., Shakovskaya,N.I., Imhoff,C.L. 1987, ApJ, 314, 297.

Walter,F.M., Brown,A., Mathieu,R.D., Myers,P.C., Vrba,F.J. 1988, AJ, 96, 297.

Figure Captions.

Figure 1. Spatial map of the sky region of Taurus-Auriga. All stars of the optical parent sample are shown as dots, and the squares represent the *Einstein* IPC fields of view in this region.

Figure 2. Distributions of spectral types (a), Hα equivalent width (b), and apparent V magnitude (c) for the stars in the optical sample (blank bins), and in the X-ray sample (hatched bins).

Figure 3. Comparison of L_x derived in this work, using REV 1 IPC data, with those published in literature, based on REV 0 data. The various symbols refer to Gahm (1980, circles), Feigelson & Kriss (1981, triangles), Feigelson & DeCampli (1981, squares), and Walter & Kuhi (1981, diamonds). Dashed segments connect different published L_x values for a given star. The solid line represents identity, and dotted straight lines represent a factor of two difference between REV 0 and REV 1 L_x. Error bars for REV 1 data (dotted) refer to statistical uncertainties alone; the typical overall uncertainty on L_x, mostly due to the absorption correction, is shown as the bar in the box in the upper left of the Figure. Note that given the size of the systematic uncertainties, differences between REV 0 and REV 1 L_x greater than a factor of two are significant.

Figure 4. X-ray luminosity function of Tau-Aur T Tauri stars, compared with those of Chamaeleon stars (Feigelson & Kriss 1989), K-M stars of the Pleiades (Micela et al. 1990), Hyades (Micela et al. 1988), young and old disk populations (Barbera et al. 1993).

Figure 5. X-ray luminosity (median, and $\pm 1\sigma$ values for each distribution) as a function of age, for the same groups of stars of Figure 4.

Figure 6. X-ray luminosity function for Tau-Aur T Tauri stars having $EW(H\alpha) > 10$ Å (solid), and $EW(H\alpha) < 10$ Å (dotted), respectively.

Figure 7. X-ray luminosity function for stars detected (solid), and not detected (dotted) at 25μ, respectively.

TABLE 1a – Summary of Data for X-Ray Detected T Tauri Stars

HBC nr.	Name	IPC Sequence	t_{exp} (sec)	Count rate (cts/sec)	S/N	A_V[a]	log L_x (erg/s)	m_v[b]	Spectral[b] Type	EW(Hα)[b] (Å)	P_{rot} (days)	Ref.	log L_{bol} ($L_\odot$)	Ref.	log $L_{\rm H\alpha}$[c] (erg/s)	log $L_{25\mu}$[d] (ergs/s)	log age (yr)	log η
32	BP Tau	4514	2679	0.009	3.7	0.84	29.90	12.09	K7	40	7.6	2	0.13	3	31.11	32.05	5.57	-0.95
34	RY Tau	4507	2247	0.014	4.3	0.55	29.71	10.01	K1	20	6.54	4	0.99	3	31.48	33.72	5.73	-2.24
35[e]	T Tau	3816	2666	0.035	7.9	1.67	30.66	9.90	K0	60	2.8	5	0.85	3	32.37	33.94	5.95	-1.58
...	...	7434	1916	0.048	...	...	...	...	...	...	...	...	...	...	...	...	...	...
36	DF Tau	10573	3529	0.009	3.5	0.55	29.81	11.49	M0	60	8.5	6	0.78	3	31.40	32.35	4.75	-0.95
38	DH Tau	3818	2664	0.025	6.0	1.52	30.12	13.92	M1	53	7	7	-0.21	3	30.80	31.85	5.71	-1.05
39	DI Tau	3818	2664	0.025	6.0	1.08	30.07	12.86	M0	2	7.7	7	0.09	3	29.65	31.63	5.61	-1.98
42	UX Tau B	7247	10563	0.052	16.1	0.57	30.29	13.67	M1	4	...	...	-0.46	3	29.47	...	6.08	...
43	UX Tau A	7247	10563	0.052	16.1	0.47	30.26	10.69	K2	3.9	2.7	8	0.03	3	30.58	32.51	6.87	-1.93
49	HL Tau	7247	10563	0.018	10.1	(0.65)[f]	30.39	14.57	K7	55	...	...	0.64	9	32.13	33.71	4.75	-1.58
50	XZ Tau	7247	10563	0.018	10.1	1.71	29.83	13.30	M3	274	...	...	0.66	3	31.70	33.08	4.74	-1.38
51	V710 Tau A	7247	10563	0.008	5.7	1.80	29.68	13.65	M1	48	...	...	-0.59	3	30.98	31.94	6.22	-0.96
55	GH Tau	4516	1965	0.015	2.7	0.25	29.67	12.95	M2	15	...	...	0.06	3	30.24	32.26	5.54	-2.02
56	GI Tau	10069	9511	0.038	13.1	1.33	30.28	13.01	K6	19	7.2	10	0.12	3	30.66	32.47	5.66	-1.81
57	GK Tau	10069	9511	0.038	13.1	0.78	30.20	12.14	K7	16	4.6	10	0.19	3	30.84	32.47	5.52	-1.63
63[e]	AA Tau	4516	1965	0.023	3.9	0.84	29.53	12.37	K7	37	8.2	7	0.02	3	30.96	32.04	5.65	-1.08
...	...	10069	9511	0.005[g]	...	...	...	...	...	...	...	...	...	...	...	...	...	...
65	DN Tau	10069	9511	0.019	9.3	0.35	30.10	12.36	M0	12	6	8	0.17	3	30.53	32.09	4.88	-1.56
77	GM Aur	3810	11156	0.010	7.1	0.10	29.75	12.03	K3	96	12.0	18	0.05	3	31.28	32.32	6.58	-1.04
79	SU Aur	3810	11156	0.056	19.8	0.64	30.64	8.93	G2	4	2.73	11	1.12	3	31.17	33.40	6.35	-2.23
80	RW Aur A	3841	1880	0.008	2.9	(0.65)[f]	29.56	10.12	K1	84	5	12	0.74	9	32.24	32.85	5.99	-0.61
81	RW Aur B	3841	1880	0.008	2.9	(0.65)[f]	29.56	12.70	K3	...	...	...	-0.26	1	...	...	7.14	...
347	032641+2420	3440	2082	0.013	3.3	0.30	29.94	12.05	K1	...	...	...	-0.30	13	29.39	<31.09	7.44	...
351	034903+2431	3175	1313	0.022	3.8	0.04	30.05	12.26	K5	1.6	$\leq$ 3.5	18	-0.30	13	29.64	<30.95	6.71	...
352	035120+3154SW	2227	2882	0.013	4.3	0.91	29.76	11.85	G0	...	...	...	-0.11	13	29.19	<30.85	7.50	...
353	035120+3154NE	2227	2882	0.013	4.3	1.03	29.78	12.31	G5	...	...	...	-0.24	13	28.79	<30.85	7.57	...
354	035135+2528NW	7408	2421	0.012	3.4	0.61	29.67	13.79	K3	...	...	...	-0.65	13	28.74	<30.85	7.53	...
355	035135+2528SE	7408	2421	0.012	3.4	0.15	29.55	12.67	K0	...	...	...	-0.51	13	28.74	<30.85	7.69	...
356	040012+2545S	7164	1978	0.011	3.2	(0.65)[f]	29.65	12.91	...	0.9	...	...	-0.78	13	28.19	<30.85	...	...
357	040012+2545N	7164	1978	0.011	3.2	0.61	29.63	12.91	K2	1.8	...	...	-0.78	13	28.19	<30.85	7.92	...
358[e]	040047+2603W	3994	2283	0.027	2.9	0.68	29.89	14.52	M2	7.8	...	...	-0.47	13	29.79	<30.85	5.93	...
...	...	7164	1978	0.011	...	...	...	...	...	...	...	...	...	...	...	...	...	...
359[e]	040047+2603E	3994	2283	0.027	2.9	0.42	29.82	14.17	M2	2.4	...	...	-0.56	13	29.38	<30.85	6.03	...
...	...	7164	1978	0.011	...	...	...	...	...	...	...	...	...	...	...	...	...	...
360	040142+2150SW	7918	3565	0.050	10.8	1.10	30.37	14.97	M3	7.6	...	...	-0.60	13	29.34	...	5.98	...
361	040142+2150NE	7918	3565	0.050	10.8	0.61	30.28	15.09	M3	5.7	...	...	-0.76	13	29.17	...	6.11	...
362	040234+2143	7918	3565	0.007	3.0	0.38	29.68	14.67	M2	4	...	...	-0.70	13	29.37	<30.85	6.20	...
372	041529+1652	9000	9132	0.006	4.6	0.00	29.48	13.26	K5	...	...	...	-0.75	13	28.27	<30.95	7.68	...
376	041559+1716	9000	9132	0.020	10.0	0.00	29.98	12.28	K7	0.7	...	...	-0.32	13	29.47	<30.95	6.31	...
379	041636+2743	3843	2066	0.021	3.6	0.76	30.25	12.37	K7	4	5.64	18	-0.01	13	29.94	<30.85	5.68	...
380	HD 283572	4507	2247	0.336	22.6	0.57	31.40	9.04	G5	...	1.548	14	0.84	13	...	<31.53	6.58	...
382	LkCa 21	4507	2247	0.014	4.3	(0.65)[f]	29.74	13.50	M3	6	...	...	0.25[h]	18	30.41	32.21	4.75	-1.80
388	042417+1744	3528	4005	0.069	10.8	0.00	30.52	10.34	K1	...	...	...	0.22	13	29.74	<30.85	6.70	...
392	042835+1700	3526	1935	0.017	3.8	0.15	29.99	12.53	K5	0.2	3.38	18	-0.37	13	29.17	<30.85	6.81	...
394	LkHα 358	7247	10563	0.018	10.1	(0.65)[f]	29.59	19.00	M5.5	47	...	...	-2.80	9	28.13	...	8.00	...
395	V710 Tau B	7247	10563	0.008	5.7	(0.65)[f]	29.55	14.60	M3	3.3	...	...	-0.46	3	29.74	...	5.40	...
397[e]	042916+1751	867	2054	0.013	3.5	0.00	29.91	12.06	K7	0.5	1.21	18	-0.18	13	29.44	<30.95	5.97	...
...	...	7247	10563	0.017	...	...	...	...	...	...	...	...	...	...	...	...	...	...

TABLE 1*a* – Continue

HBC nr.	Name	IPC Sequence	t_{exp} (sec)	Count rate (cts/sec)	S/N	A_V[a]	log L_x (erg/s)	m_v[b]	Spectral[b] Type	EW(Hα)[b] (Å)	P_{rot} (days)	Ref.	log L_{bol} ($L_\odot$)	Ref.	log $L_{\mathrm{H}\alpha}$[c] (erg/s)	log $L_{25\mu}$[d] (ergs/s)	log age (yr)	log η
399	V827 Tau	7247	10563	0.044	15	0.61	30.53	12.18	K7	1.8	3.63	15	0.04	13	30.03	<31.15	5.65	...
400	V826 Tau	7247	10563	0.036	14.5	0.53	30.42	12.11	K7	1.6	4.05	15	-0.30	13	29.27	<31.15	6.09	...
403	042950+1757	3819	2644	0.016	4.3	0.91	30.15	13.22	K7	0.7	...	...	-0.36	13	29.49	<30.85	6.33	...
404	V807 Tau	4516	1965	0.015	2.7	(0.65)[f]	29.55	11.22	K7	13	...	...	-0.12[h]	19	30.53	...	5.90	...
405	V830 Tau	10069	9511	0.026	9.6	0.42	30.25	12.21	K7	3	2.76	15	-0.05	13	29.79	<31.20	5.70	...
407	043124+1824	3819	2644	0.009	2.8	1.22	29.93	12.67	G8	...	...	...	-0.30	13	29.19	<30.85	7.63	...
426	LkCa 19	3810	11156	0.013	8.1	(0.65)[f]	29.81	10.85	K0	1	2.24	18	0.20	13	29.95	<31.09	6.81	...
427	045251+3016	3810	11156	0.026	11.8	0.00	30.10	11.60	K7	0.7	4.70	18	0.01	13	29.73	31.72	5.67	-2.00
429	V836 Tau	2684	1697	0.011	3.2	0.91	29.99	13.13	K7	9	6.99	15	-0.15	13	30.14	31.61	5.95	-1.47

NOTES.– Many of the X-ray sources appearing in the Table have two (or three) T Tauri counterparts. Tabulated count rates refer to the X-ray source, and have been divided by the number of counterparts to yield the L_x in the last column. Unresolved pairs are: (RY Tau/LkCa 21), (DH/DI Tau), (UX Tau A/B), (V710 Tau A/B), (GH/V807 Tau), (GI/GK Tau), (RW Aur A/B), (035120+3154 SW/NE), (035135+2528 NW/SE), (040012+2545 S/N), (040047+2603 W/E), (040142+2150 SW/NE), and (HL Tau, XZ Tau, LkHα 358).

a) A_V from Strom et al. 1989 (detections) and Cohen & Kuhi 1979 (upper limits); *b*) m_v, spectral types, and EW(Hα) from Herbig & Bell 1988, except for m_v of HBC 382 (Martin et al. 1994) and HBC 404 (Bouvier et al. 1993); *c*) $L_{\mathrm{H}\alpha}$ derived from literature data, as described in Paper II; *d*) $L_{25\mu}$ is the luminosity in the 16-30μ band, derived from $f_{25\mu}$ listed by Strom et al. 1989; *e*) Source detected in two different IPC images, free from detector ribs occultation. In these cases a Maximum Likelihood method was used to derive the L_x (and S/N) listed in the Table; *f*) A_V not found in literature; the average A_V for other detections has been adopted in the derivation of count-rate to flux conversion factor; *g*) Source detected with the Local method in the Broad band; *h*) L_{bol} derived from m_v and bolometric correction; *i*) A_V not found in literature; the average A_V for other upper limits has been adopted in the derivation of count-rate to flux conversion factor.

REFERENCES.– (1) Herbig & Bell 1988; (2) Vrba et al. 1984; (3) Cohen, Emerson & Beichman 1989; (4) Red'kina & Zausaeva 1987; (5) Herbst et al. 1986; (6) Bouvier & Bertout 1989; (7) Rydgren et al. 1985; (8) Bouvier et al. 1986; (9) Cohen & Kuhi 1979; (10) Vrba et al. 1986; (11) Herbst et al. 1987; (12) Herbig 1962; (13) Walter et al. 1988; (14) Walter et al. 1987; (15) Rydgren et al. 1984; (16) Walter 1986; (17) Praderie et al. 1986; (18) Bouvier et al. 1993; (19) Martin et al. 1994.

TABLE 1*b* – Summary of Data for T Tauri Stars with X-Ray Upper Limits

HBC nr.	Name	IPC Sequence	t_{exp} (sec)	Count rate (cts/sec)	A_V[a]	log L_x (erg/s)	m_v[b]	Spectral[b] Type	EW(Hα)[b] (Å)	P_{rot} (days)	Ref.	log L_{bol} ($L_\odot$)	Ref.	log $L_{\mathrm{H}\alpha}$[c] (erg/s)	log $L_{25\mu}$[d] (ergs/s)	log age (yr)	log η
26	FP Tau	3815	1571	<0.013	0.26	<29.93	13.9	M4	38	...	...	-0.27	3	30.30	31.68	5.00	-1.38
27	CX Tau	3815	1571	<0.014	0.85	<30.08	13.72	M2.5	20	...	...	-0.17	3	30.25	31.85	4.75	-1.60
33	DE Tau	3843	2066	<0.010	0.20	<29.81	13	M2	54	7.6	18	-0.14	3	30.77	32.15	4.75	-1.38
37	DG Tau	10573	3529	<0.008	(1.28)[i]	<29.89	12.01	M	113	6.3	18	0.88	9	31.71	33.62	4.75	-1.91
41	IQ Tau	3818	2664	<0.012	0.77	<30.01	13.3	M0.5	7.8	...	...	-0.18	3	29.98	32.13	5.82	-2.15
52	UZ Tau e	4515	1986	<0.025	0.85	<30.33	12.86	M1	82	...	...	-0.07	3	31.44	32.53	5.59	-1.09
53	UZ Tau w	4515	1986	<0.025	1.53	<30.43	14.6	M3	80	...	...	-0.38	3	31.31	...	5.18	...
54	GG Tau	867	2054	<0.013	0.78	<30.04	12.24	K7	54	10.3	18	0.12	3	31.22	32.53	5.58	-1.31
58	DL Tau	4515	1986	<0.010	(1.28)[i]	<30.00	13.05	K7	105	9.4	18	0.17	9	31.31	32.43	5.54	-1.12
60	HN Tau	867	2054	<0.015	0.54	<30.06	13.7	K5	139	...	...	-0.48	3	30.93	32.55	7.09	-1.62
62	DM Tau	10538	2614	<0.010	0.00	<29.66	13.99	M1	139	...	...	-0.77	3	30.70	31.82	6.77	-1.11
78	AB Aur	3810	11156	<0.056	0.65	<30.64	7.07	B9	27	1.88	17	1.78	3	32.65	...	6.56	...
386	FV Tau	10572	3327	<0.008	4.83	<29.69	15.4	K5	23	...	...	0.41	3	31.32	32.78	5.49	-1.45
387	FV Tau/c	10572	3327	<0.008	3.49	<29.82	17.2	M3.5	20	...	...	-0.32	3	30.44	...	5.04	...
393	L1551/IRS 5	7247	10563	<0.003	(1.28)[i]	<29.32	...	K2	...	...	...	...	...	...	...	...	...
406	HN Tau/c	867	2054	<0.015	0.54	<30.18	18.1	M	89	...	...	...	...	...	...	...	...

NOTES AND REFERENCES as in Table 1*a*.

Figure 1

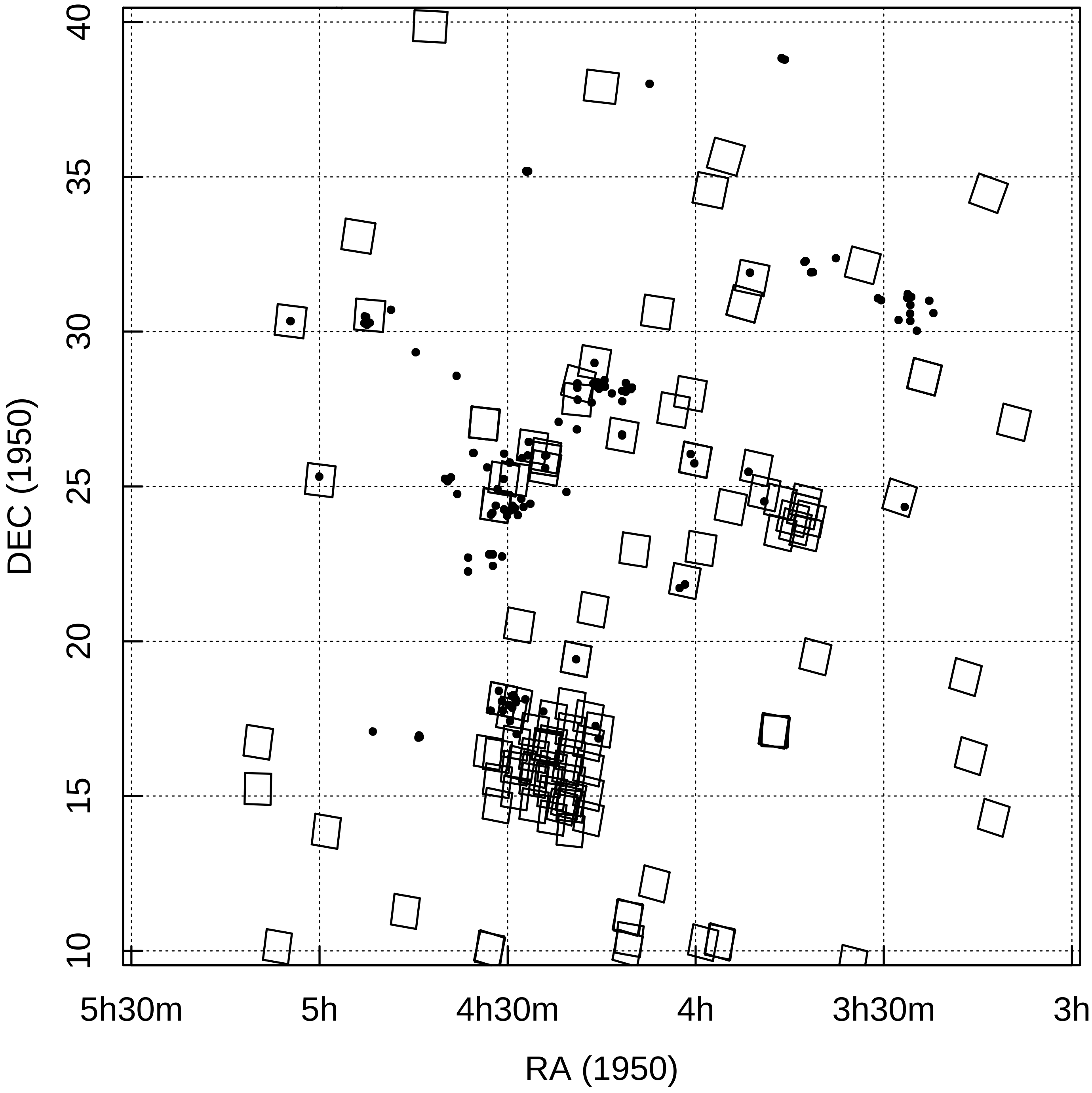

Figure 2a

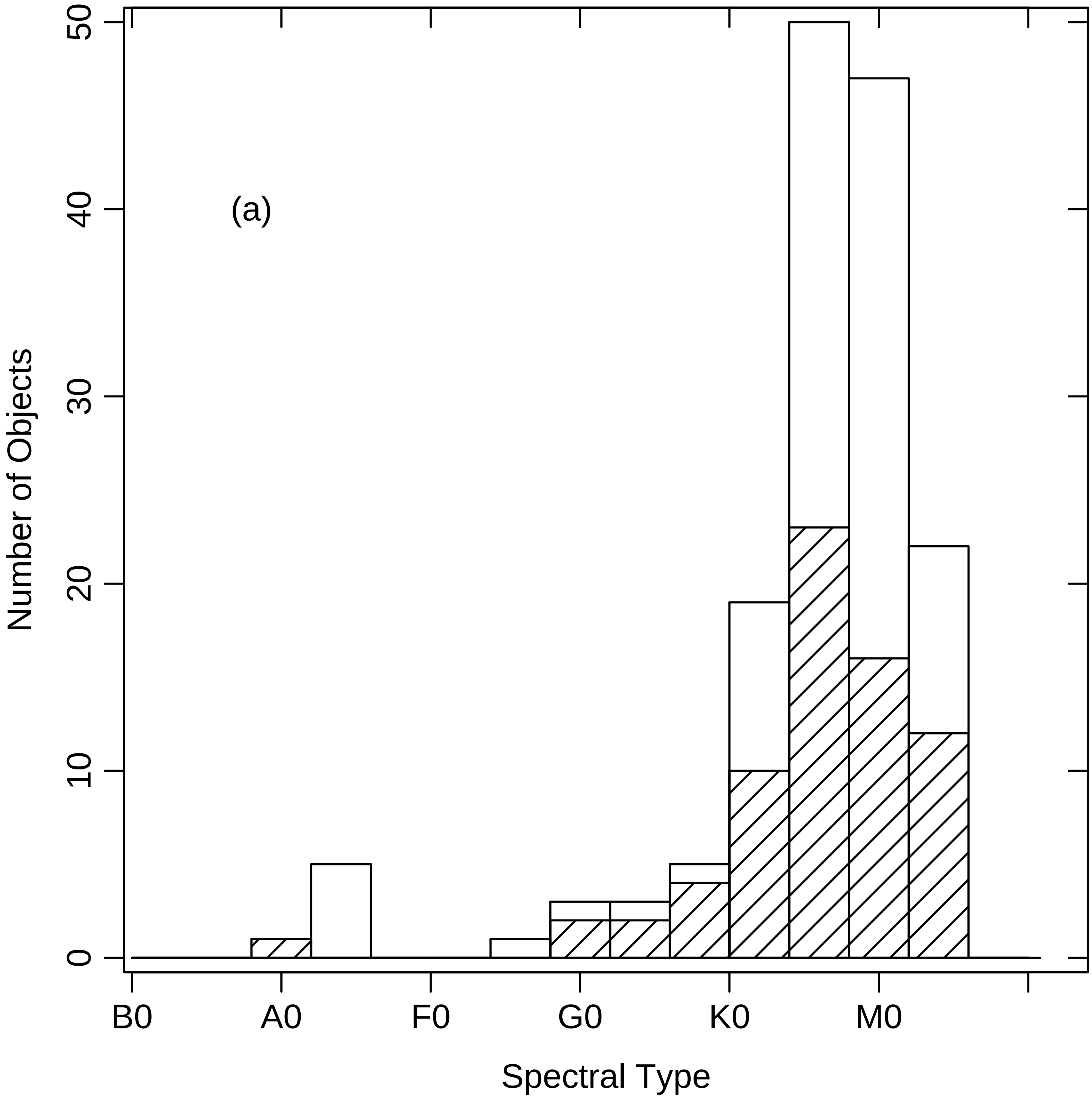

(a)
Number of Objects
0
10
20
30
40
50
B0
A0
F0
G0
K0
M0
Spectral Type

Figure 2b

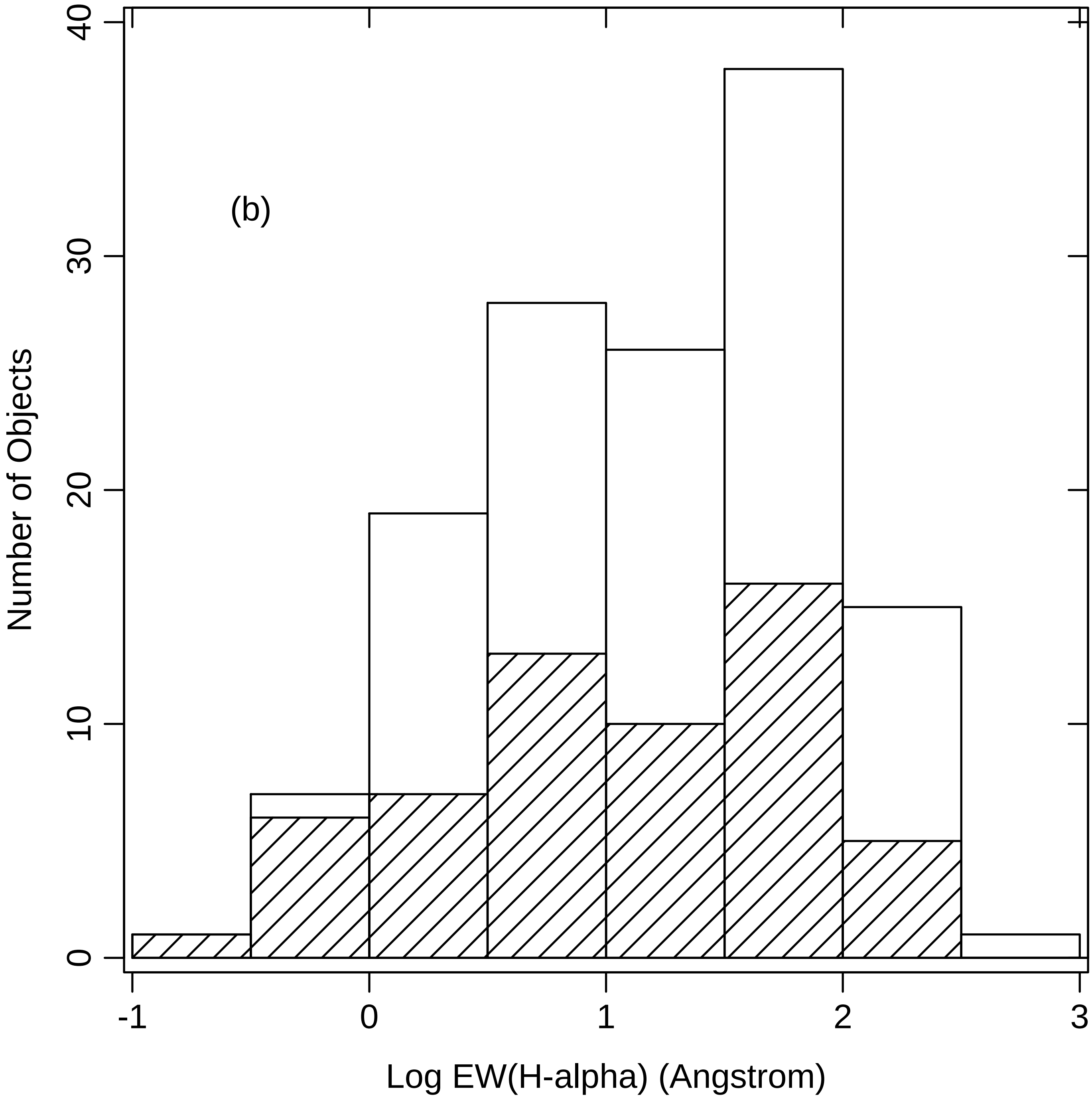

Figure 2c

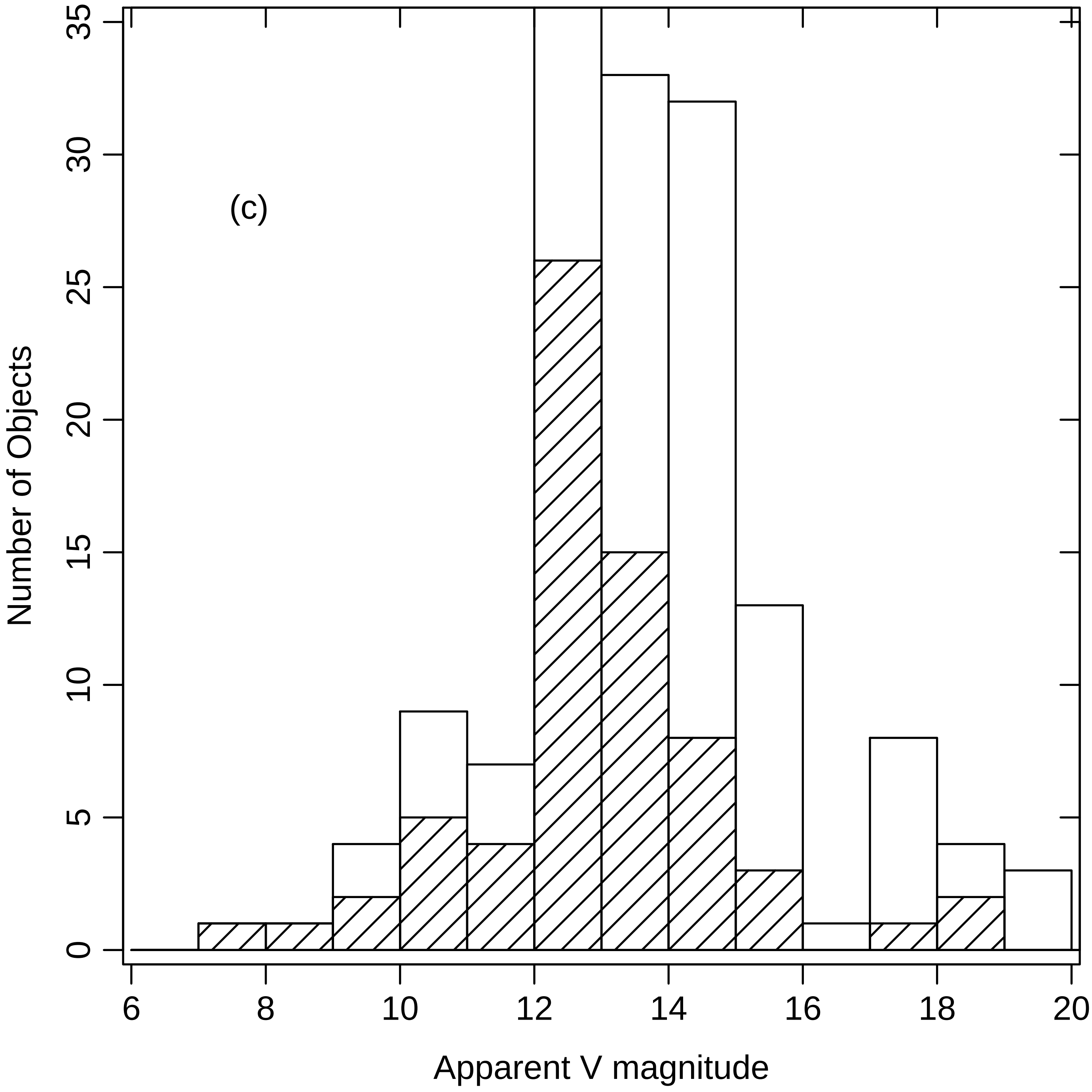
(c)
Number of Objects
Apparent V magnitude
0
5
10
15
20
25
30
35
6
8
10
12
14
16
18
20

Figure 3

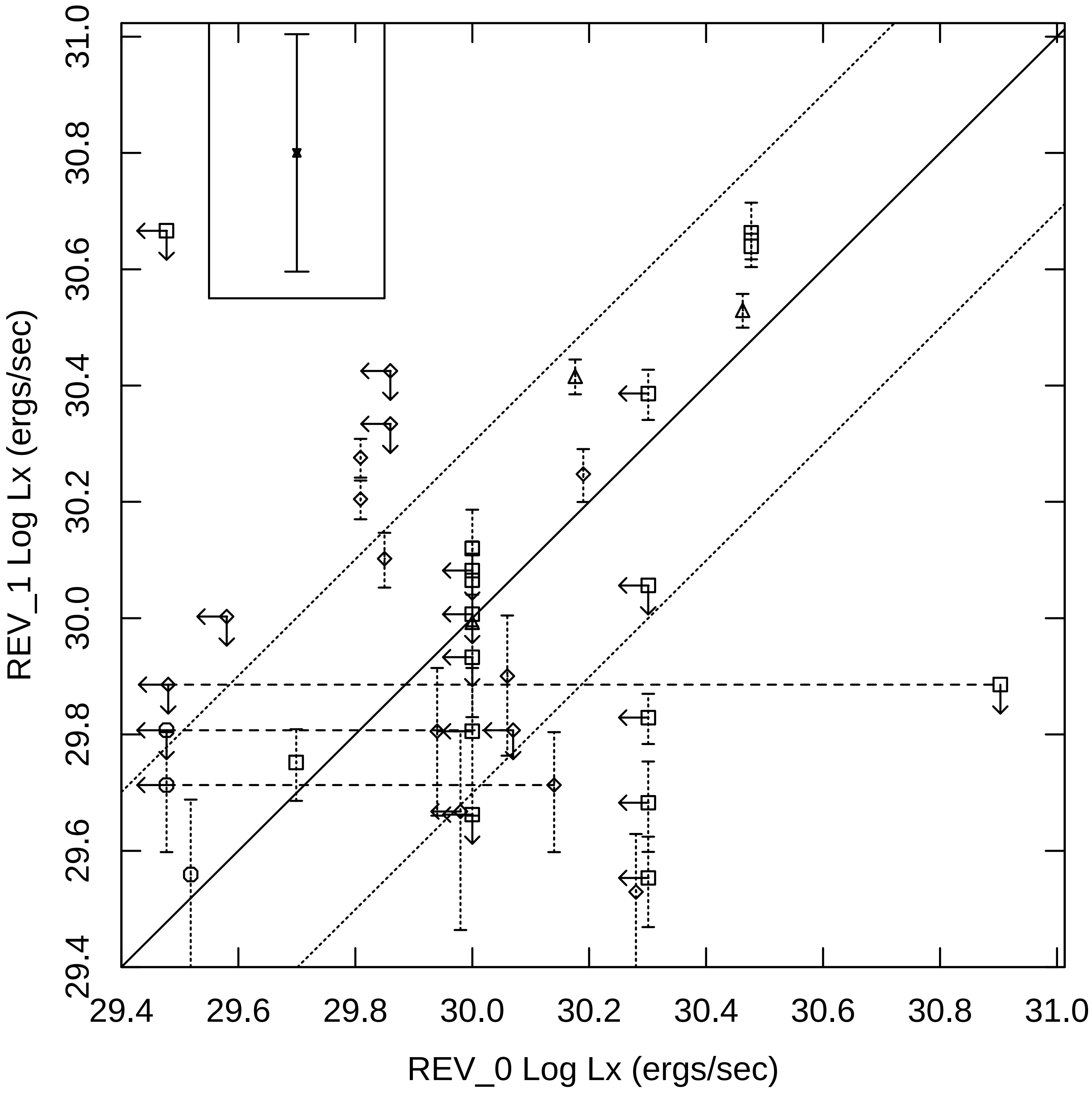

31.0
30.8
30.6
30.4
30.2
30.0
29.8
29.6
29.4
REV_1 Log Lx (ergs/sec)
29.4
29.6
29.8
30.0
30.2
30.4
30.6
30.8
31.0
REV_0 Log Lx (ergs/sec)

Figure 4

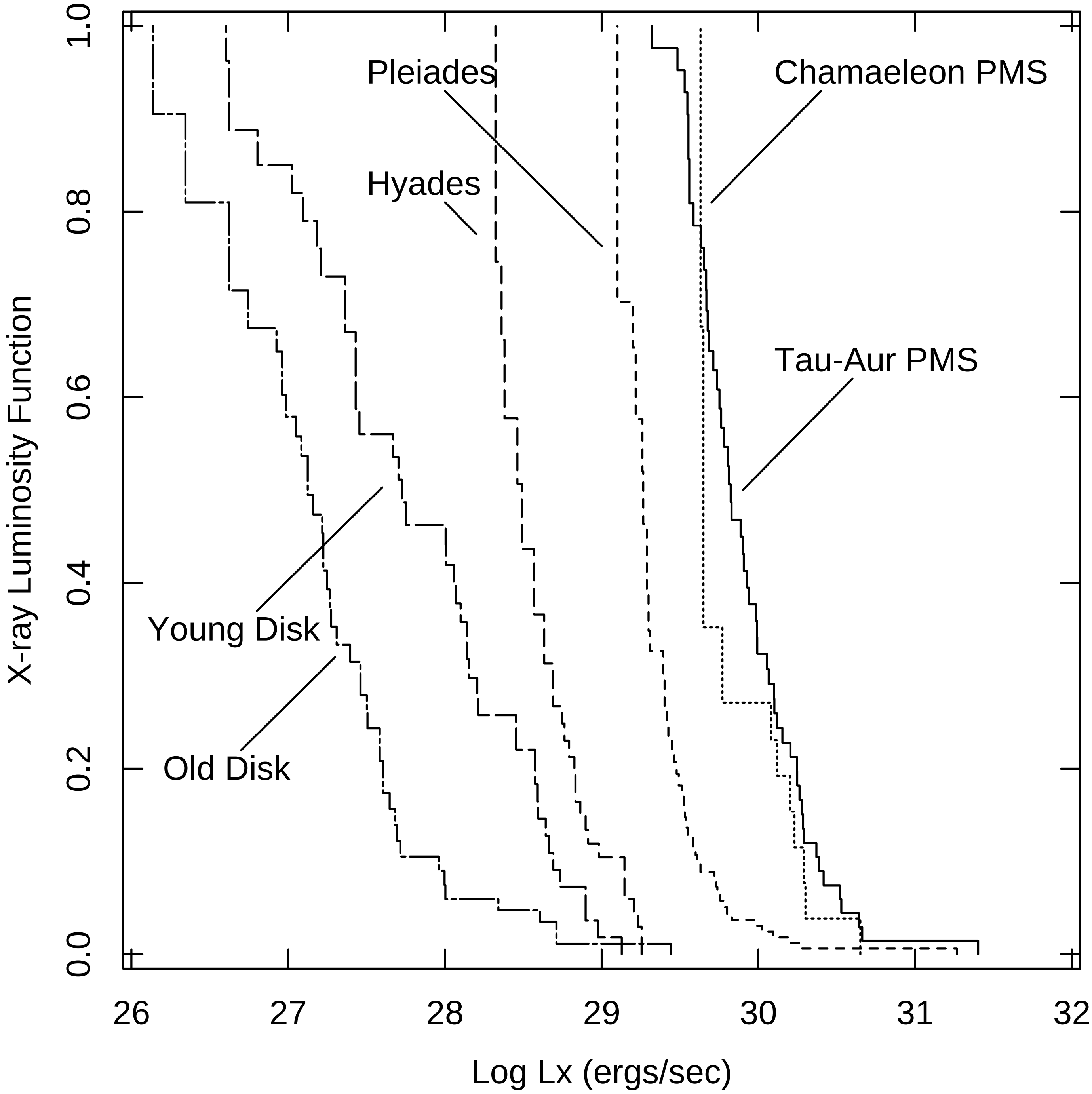
Pleiades
Chamaeleon PMS
Hyades
Tau-Aur PMS
Young Disk
Old Disk
X-ray Luminosity Function
0.0
0.2
0.4
0.6
0.8
1.0
26
27
28
29
30
31
32
Log Lx (ergs/sec)

Figure 5

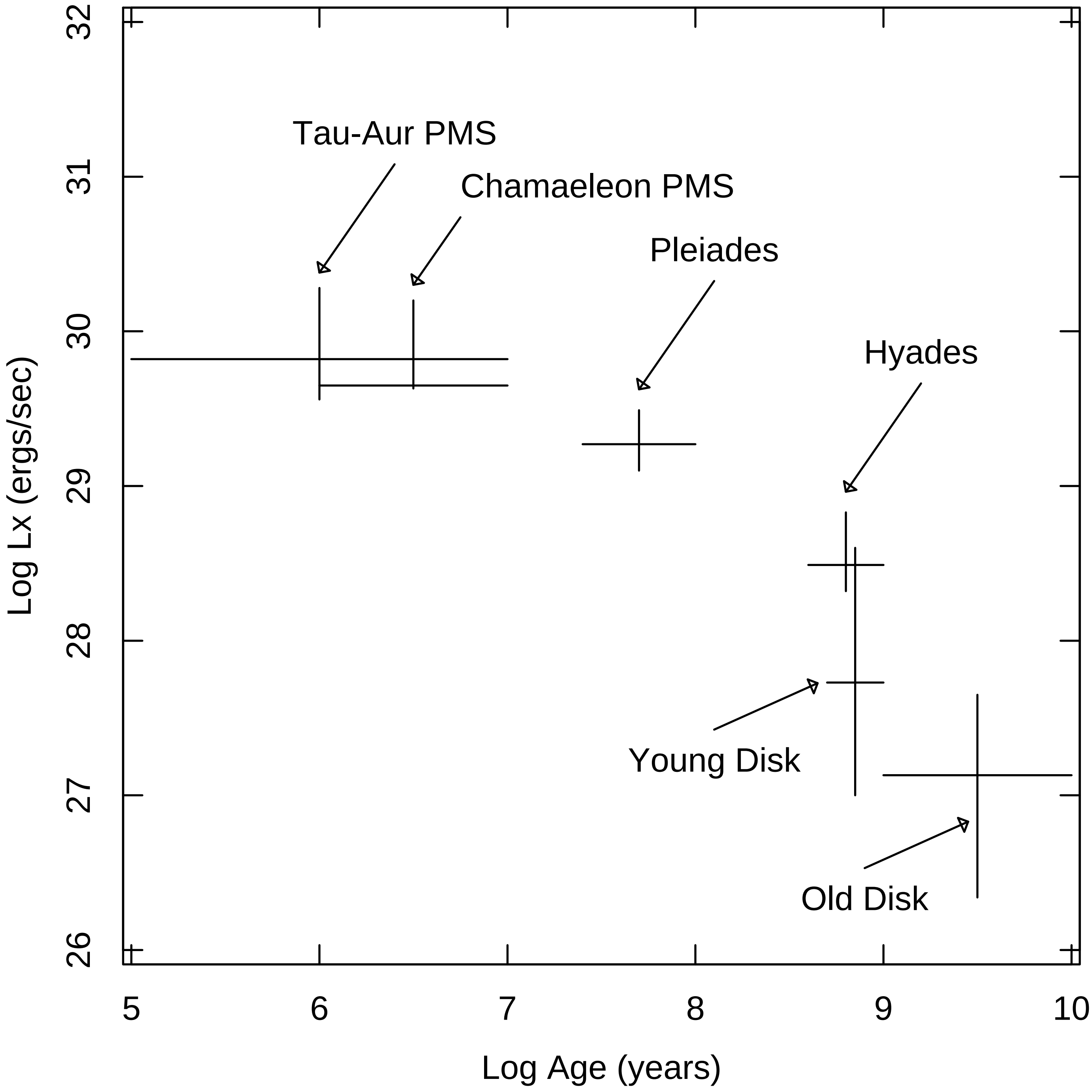
Tau-Aur PMS
Chamaeleon PMS
Pleiades
Hyades
Young Disk
Old Disk
Log Lx (ergs/sec)
26
27
28
29
30
31
32
5
6
7
8
9
10
Log Age (years)

Figure 6

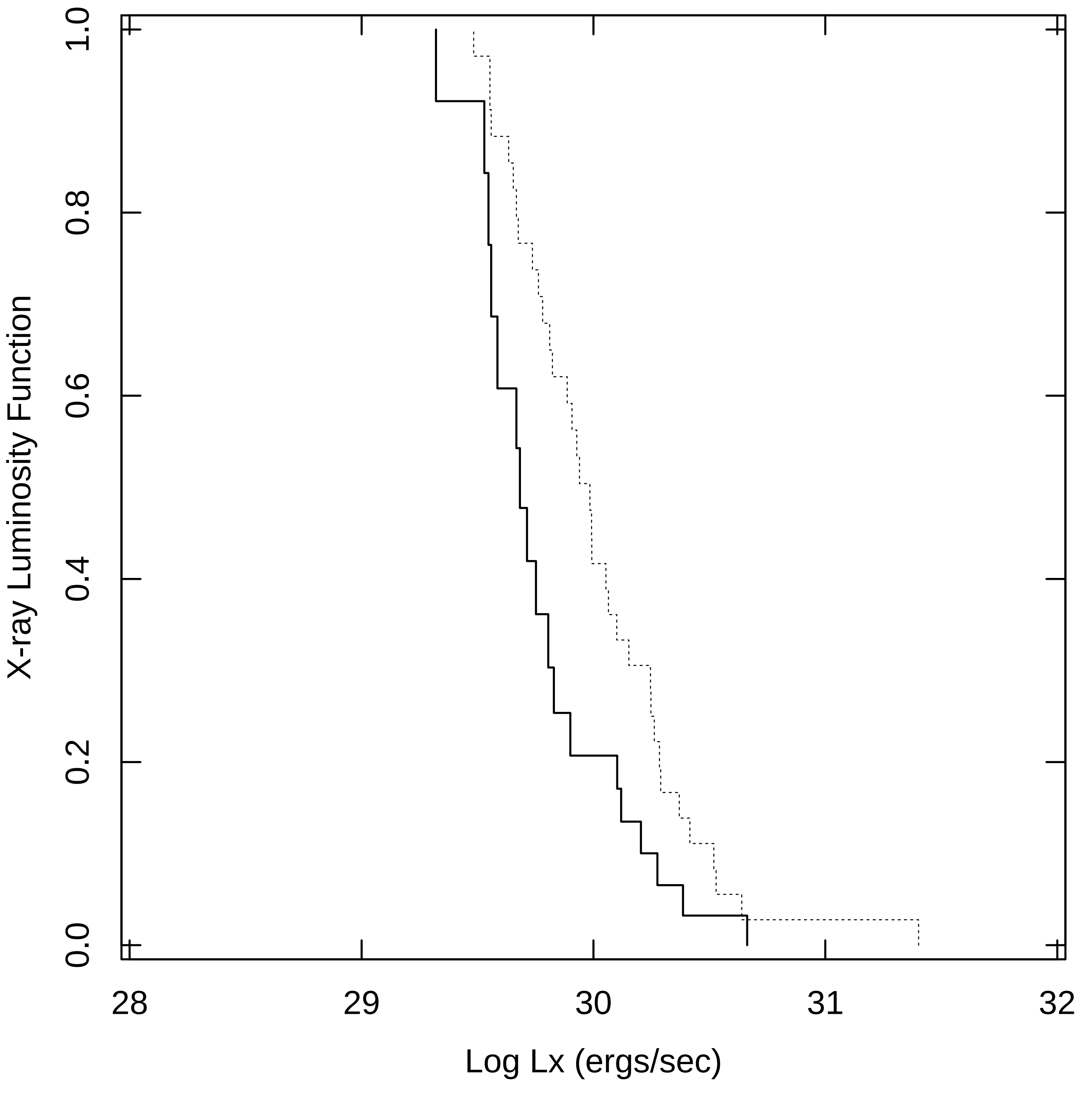
X-ray Luminosity Function
0.0
0.2
0.4
0.6
0.8
1.0
28
29
30
31
32
Log Lx (ergs/sec)

Figure 7

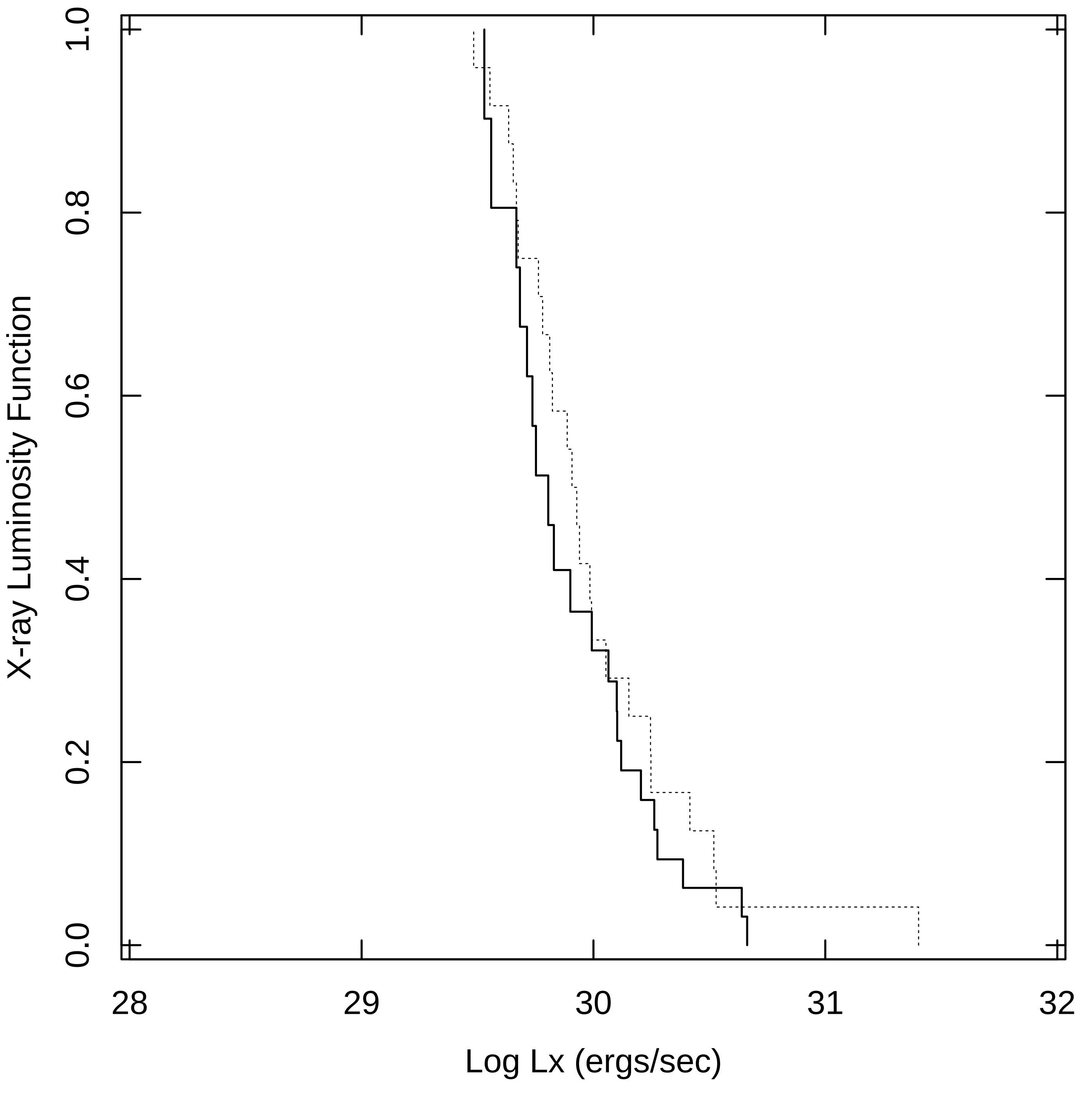
X-ray Luminosity Function
0.0
0.2
0.4
0.6
0.8
1.0
28
29
30
31
32
Log Lx (ergs/sec)